Bandwidth Enhancement of Proximity-Coupled Patch Antenna Using Dual Open-Ended Ring-Shaped Slots for Sub-6 GHz Applications

Rheyuniarto Sahlendar Asthan[1*], Mia Maria Ulfah[2]

[1]*Department of Electrical Engineering, Institut Teknologi Sumatera*
Jalan Terusan Ryacudu, Desa Way Huwi, Kecamatan Jati Agung, Lampung Selatan 35365, Indonesia

[2]*Department of Telecommunication Engineering, Institut Teknologi Sumatera*
Jalan Terusan Ryacudu, Desa Way Huwi, Kecamatan Jati Agung, Lampung Selatan 35365, Indonesia

[*]*Corresponding author. Email: rheyuniarto.asthan@el.itera.ac.id*

Abstract— This paper presents a bandwidth enhancement of patch antenna intended for sub-6 GHz applications. A square-shaped radiating patch is configured on a double-layer FR-4 dielectric substrates with a dielectric constant of 4.3 and a total thickness of 3.2 mm. To improve the impedance bandwidth, the antenna is fed using proximity-coupling method, in which the microstrip feeding line and the ground plane are placed on the top and bottom layers of the second substrate. Dual open-ended ring-shaped slots are subsequently introduced and etched on the radiating patch element to further enhance the antenna bandwidth. Various slot structures are evaluated, and their physical parameters are varied in a parametric study to analyze their effect on antenna performance, particularly impedance bandwidth. The proposed antenna has a compact dimension of $0.38\lambda_0 \times 0.38\lambda_0 \times 0.06\lambda_0$ and exhibits wideband characteristics with a fractional bandwidth of 22.3%.

Keywords— open-ended ring-shaped slot, proximity coupling, sub-6 GHz applications, wideband patch antenna

I. Introduction

The sub-6 GHz band has been widely utilized in modern telecommunication systems, including wireless local area networks, 5G, and Internet of Things (IoT) applications. This spectrum offers a favorable trade-off between wide coverage and high data rates, as well as better propagation characteristics, such as lower path loss and better signal penetration compared to higher-frequency bands [1]. In these systems, antennas play a fundamental role in enabling signal transmission and reception. With the rapid growth of wireless communication technologies, there is an increasing demand for more compact and efficient antenna designs. In response to this need, microstrip antennas, also known as patch antennas, have emerged as a promising solution.

Patch antennas offer many attractive features including low profile, lightweight, low fabrication cost, and seamless integration with planar circuits. However, the conventional patch antennas suffer from several drawbacks, such as low efficiency and high Q-factor, which result in a narrow impedance bandwidth [2]. These drawbacks limit their suitability for wideband communication systems. In particular, the narrow bandwidth characteristic becomes a critical issue, as modern wireless applications require antennas to operate over broader frequency ranges to support higher data rates and multiple operating bands within a single structure.

Various bandwidth enhancement methods for patch antennas have been reported in recent literature. Common approaches include the use of U-slots [3], [4], parasitic patches [5], [6], defected ground structures [7], [8], as well as their combinations [9]. In addition to these methods, several alternative methods have also been explored such as the use of complex slot geometries [10], shorting pins or vias [11], aperture-coupled feeding [12], and metamaterial- or metasurface-based structures [13]. Although these methods can effectively improve the impedance bandwidth, they often introduce several trade-offs. For instance, the U-slot method generally exhibits more complex surface current distributions due to its slot geometry, making the impedance matching optimization more challenging. Meanwhile, the inclusion of parasitic elements and metamaterial- or metasurface-based structures commonly increases the antenna dimensions due to the additional resonating elements or unit-cell layers. In addition, the antenna performance in metamaterial- or metasurface-based structures strongly depends on the number of unit cells, where increasing the number of cells may further increase the structural complexity of the antenna. The use of shorting pins or vias may also increase fabrication complexity because of alignment sensitivity, particularly in multilayer configurations. Moreover, unwanted back radiation introduced by defected ground structures, which also serve as additional radiating elements, may reduce the antenna directivity and consequently degrade the gain performance. A similar drawback is also observed in aperture-coupled feeding methods, where a slot in the ground plane is required as an electromagnetic coupling aperture between the feed line and the radiating patch. Alternatively, some designs employ a proximity-coupled feeding method [14], [15], due to its merits, such as low spurious radiation and the ability to provide wider bandwidth, generally exceeding 10%.

In this paper, a proximity-coupled patch antenna incorporating dual open-ended ring-shaped slots is presented. The antenna is designed to operate in the sub-6 GHz frequency range. The proposed configuration is introduced to improve the

Received 11 April 2026, Revised 17 May 2026, Accepted 20 May 2026.
DOI: https://doi.org/10.15294/jte.v18i1.47475

impedance bandwidth while maintaining a relatively simple antenna structure. By carefully optimizing the slot dimensions and feeding configuration, the antenna achieves enhanced bandwidth performance without significantly affecting its radiation pattern characteristics. The design is intended to provide a compact and efficient solution suitable for modern sub-6 GHz applications. The main contributions of this work are as follows. First, a bandwidth enhancement method is proposed by combining a proximity-coupling feeding method with the incorporation of dual open-ended ring-shaped slots in the radiating element. The proposed configuration excites additional resonant frequencies and enables easier impedance matching optimization, thereby improving the fractional bandwidth without increasing antenna complexity and maintaining a low-profile structure. Second, this work presents a parametric investigation into the effects of slot geometry on antenna performance, providing practical insights for bandwidth optimization in sub-6 GHz patch antennas.

II. Method

A. Wideband Antenna Configuration

In achieving wideband characteristic, the proposed antenna is developed through two sequential stages. First, a patch antenna fed using a proximity-coupling method is designed as the initial structure, and subsequently the antenna is further developed by modifying the radiating patch using dual slots, as illustrated in Figures 1 and 2, respectively. In this configuration, the patch antenna consists of two dielectric substrates, each with a thickness (t) of 1.6 mm and the same length (L) and width (W) of 21.6 mm. The material employed for the design is FR-4 with a dielectric constant of 4.3 and tan-δ of 0.02. Moreover, a square-shaped radiating patch with a length (l_p) and width (w_p) of 10.8 mm is placed on the top side of the first substrate, while the feedline and ground plane are arranged on the top and bottom sides of the second substrate, respectively. This structure enables electromagnetic coupling between the feedline and the radiating patch, thereby reducing spurious radiation from the feedline and enhancing the impedance bandwidth of the antenna compared to conventional patch antennas using the microstrip feeding-line method [16]. To achieve $|S_{11}|$ below -10 dB, the feedline width (w_f) and coupling feedline length (l_d) are adjusted.

Subsequently, without altering the antenna structure from the initial design, the radiating patch is modified by introducing dual square open-ended ring-shaped slots arranged with a certain spacing (d_s). In the design, the length of the outer slot (l_s) is chosen to be approximately half of the radiating patch length. The inclusion of slots on the radiating patch alters the effective current distribution of the antenna by forcing the surface current to flow around the slot edges, as indicated by the maximum current marked with red arrows in Figure 3 (bottom), rather than predominantly in the vertical direction along the original direct path observed in the antenna without slots, shown in Figure 3 (top). As a result, the effective current path length increases, producing additional inductive and capacitive effects that introduce an additional resonant frequency. Through fine tuning of the slot configuration, the induced resonant frequency can be adjusted to occur near the fundamental resonant frequency, thereby enhancing the fractional bandwidth of the patch antenna.

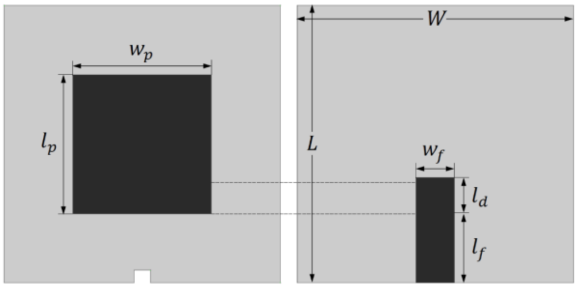

Figure 1. Geometry of proximity-coupled patch antenna.

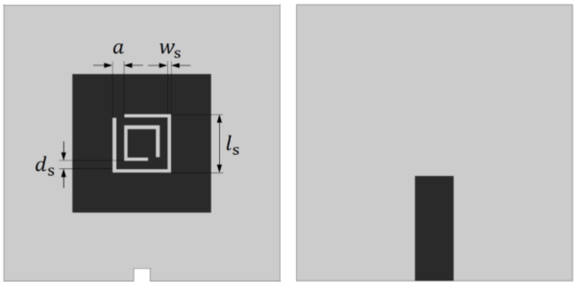

Figure 2. Geometry of proximity-coupled patch antenna with dual open-ended ring-shaped slots.

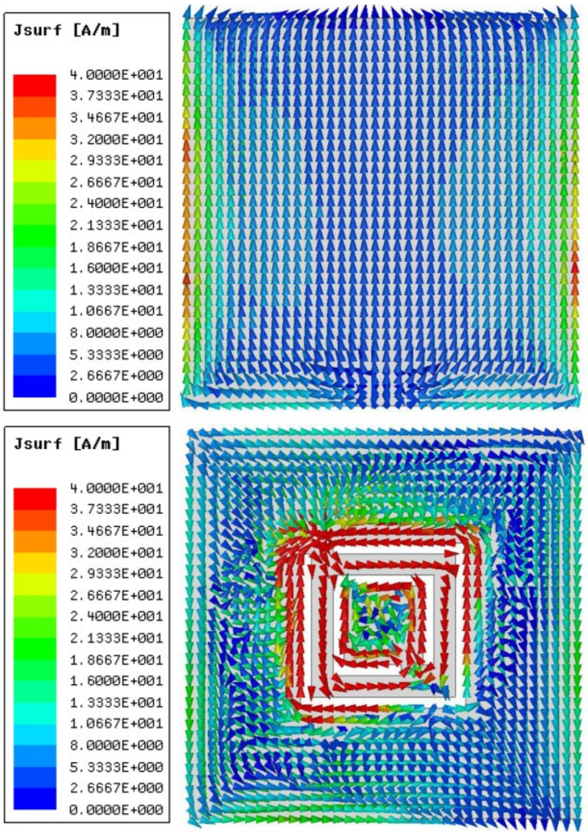

Figure 3. Surface current distribution of patch antenna without slots (top) and with slots (bottom) at the frequency of 5.8 GHz.

To investigate the frequency response and impedance matching related to the operating bandwidth of the proposed patch antenna, different positions of the open-ended slot structures are evaluated as depicted in Figure 4(a), and the corresponding results are presented in Figure 4(b). The selection of these structures is based on the electromagnetic coupling generated between the open-ended ring-shaped slots, including the inner and outer slots, as well as its interaction with the radiating patch of the antenna. The position of the open-ended sections influences the surface current distribution and the coupling strength between the slots, thereby affecting the induced resonant frequencies and matching impedance. When the open-ended structures are symmetrically arranged at the bottom side of both the inner and outer slots, i.e., Ant. A, dual resonant frequencies are observed. The second resonant frequency in the higher frequency region shifts toward the lower frequency region when the open-ended structures are located on opposite sides of both slots, referred to as Ant. B, due to the increased effective current path along the slot structures. In contrast, for Ant. C and Ant. D, where the open-ended structures are positioned at the slot edges in opposite directions, an additional resonant frequency is excited between the first two resonances due to the change in coupling characteristics between the slots, resulting in an improved impedance bandwidth of the antenna. Similarly, for Ant. E, where both open-ended structures are arranged on the same edge side of the slots, the frequency response shifts to the higher frequency region, attributed to the concentration of the current distribution at the slot edges. Given that Ant. D provides the widest impedance bandwidth, this structure is adopted for further design optimization.

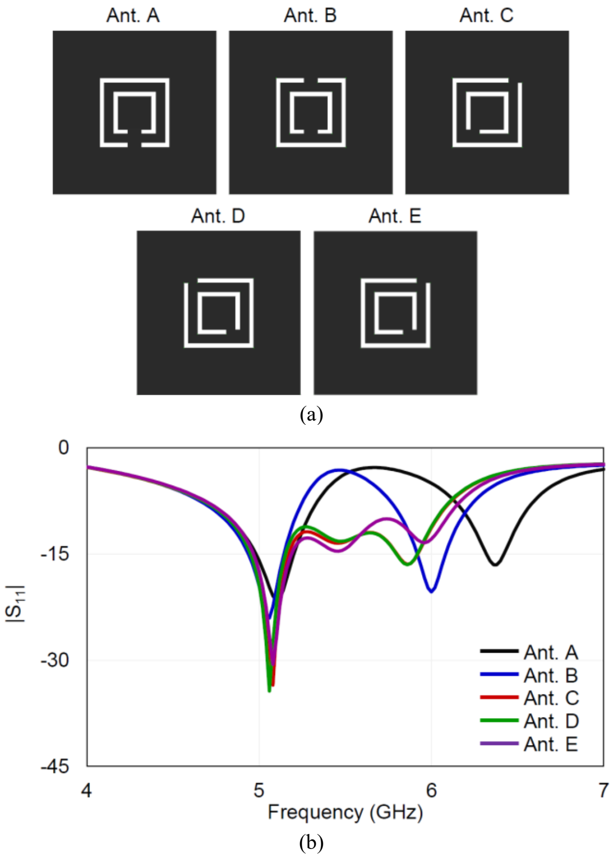

Figure 4. Performance comparison of the proximity-coupled patch antenna with different open-ended ring-shaped slot designs, (a) slot geometry, (b) simulated $|S_{11}|$.

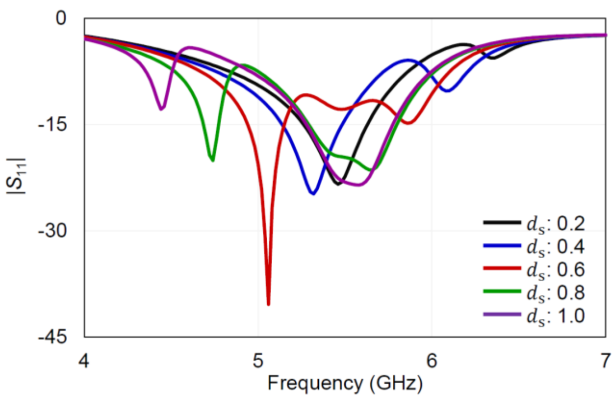

Figure 5. Effect of slot spacing (unit mm) on the performance of the proposed proximity-coupled patch antenna.

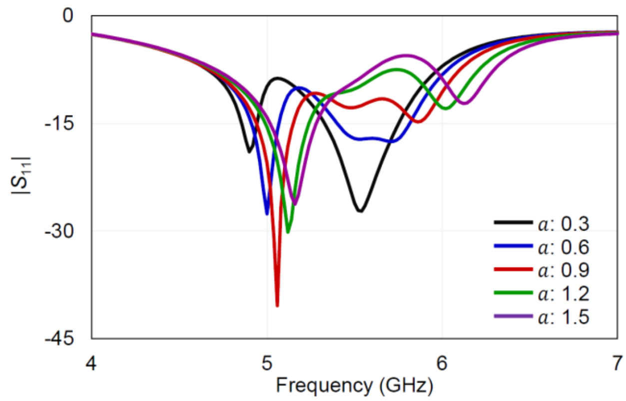

Figure 6. Effect of open-ended slot length (unit mm) on the performance of the proposed proximity-coupled patch antenna performance.

A. Parametric Study

In this work, a parametric study of the open-ended square slots and feedline geometries is conducted to optimize the impedance bandwidth of the proposed patch antenna. The study includes slot spacing, open-ended slot length, and the coupling feedline length.

1) Slot Spacing

The coupling effect between the dual open-ended ring-shaped slots over the radiating patch is investigated by varying the slot spacing (d_s) from 0.2 mm to 1.0 mm with an interval of 0.2 mm. The results depicted in Figure 5 show that the variation of d_s significantly affects the resonant frequency response and impedance matching characteristics of the antenna. As the slot spacing increases, the mutual coupling between the slots decreases, resulting in a shift of both resonant frequencies toward the lower frequency region. For larger spacing values, particularly d_s = 0.8 mm and d_s = 1.0 mm, the first resonant frequency exhibits degraded impedance matching, as indicated by the higher $|S_{11}|$. In contrast, for the other spacing values, the first resonant frequency achieves better impedance matching compared to the higher resonant frequency. Based on this parametric study, d_s = 0.6 mm provides the widest impedance bandwidth.

2) Open-Ended Slot Length

Based on the simulation results shown in Figure 4(b), the slot configuration, particularly the position of the open-ended section in the slot structure, significantly influences the $|S_{11}|$ characteristics and the frequency response of the antenna. Therefore, to further examine its effect, the open-ended slot length (a) is analyzed by varying its value from 0.3 mm to 1.5 mm as depicted in Figure 6. It should be noted that, in this study, the variation of the open-ended slot length is applied to both ring-shaped slots, including the inner and outer slots. The variation of a also causes a slight shift in the first resonant frequency and changes the impedance matching at both resonances. The most noticeable effect is observed at the higher resonant frequency excited by the slots, which tends to shift toward higher frequencies with increasing a due to the change in the effective current path length. At this resonant frequency, the impedance matching gradually degrades for larger values of a. In addition, it can be observed that a particular value of the open-ended slot length induces an additional resonant frequency around 5.5 GHz, particularly for a = 0.6 mm and a = 0.9 mm, which is gradually suppressed as the value increases.

3) Coupling Feedline Length

The final parametric study is conducted by varying the coupling feedline length (l_d). As ring-shaped slots are introduced on the radiating patch to enhance the antenna bandwidth, it is necessary to investigate the effect of the coupling feedline length on the proposed patch antenna with the inclusion of slots, particularly in terms of impedance matching. From the results plotted in Figure 7, the variation of l_d mainly affects the $|S_{11}|$, while the resonant frequencies remain almost unchanged. This behavior can be observed at both the lower and higher resonant frequencies at 5.06 GHz and 5.85 GHz, respectively. As the value of l_d increases, the $|S_{11}|$ at the lower resonant frequency degrades, whereas at the higher resonant frequency the $|S_{11}|$ improves. The opposite behavior is observed when l_d is decreased. This demonstrates that variations in l_d alters the coupling between the feedline, the radiating patch, and the slots, which consequently affects the impedance characteristics at both resonant frequencies. As the value of l_d increases toward 3.6 mm, the feedline becomes positioned below the outer ring-shaped slot, resulting stronger coupling between and improved matching impedance at the resonant frequency induced by the slots. However, this condition inversely causes the impedance matching between the radiating patch and the feedline to degrade. The physical parameters of the proposed proximity-coupled patch antenna after the parametric study are presented in Table I.

III. Results and Discussion

A. Performance Comparison

Figures 8-10 present the performance comparison of the proposed proximity-coupled patch antenna with and without slots in terms of frequency response and $|S_{11}|$, radiation patterns, and boresight gain, respectively. From the results shown in Figure 8, the proximity-coupled patch antenna without slots achieves a fractional bandwidth of 12.3%, ranging from 5.39 GHz to 6.10 GHz. This bandwidth is significantly wider than a conventional patch antenna fed by a microstrip line, which typically exhibits a bandwidth less than 5% [16]. Moreover, the inclusion of dual open-ended ring-shaped slots provides a fractional bandwidth of 22.3%, covering the operating frequency range of 4.82 GHz to 6.03 GHz. The wideband characteristic of the proposed proximity-coupled patch antenna is achieved through the excitation of additional resonant modes at 5.06 GHz and 5.48 GHz by the slot structures. As discussed in Section II, the open-ended ring-shaped slots modify the surface current distribution on the radiating patch, generating resonances close to the fundamental mode. The interaction among these adjacent resonances broadens the impedance bandwidth while reducing the overall Q-factor, thereby improving the fractional bandwidth. The bandwidth of the proposed antenna improves by about 81.3% compared to the proximity-coupled patch antenna without slots.

TABLE I. Physical Parameter of the Proposed Patch Antenna

Parameter	Value (mm)	Parameter	Value (mm)
L	21.6	t	3.2
W	21.6	l_d	3.0
l_p	10.8	l_s	4.6
w_p	10.8	w_s	0.3
w_f	3.0	d_s	0.6
l_f	5.4	a	0.9

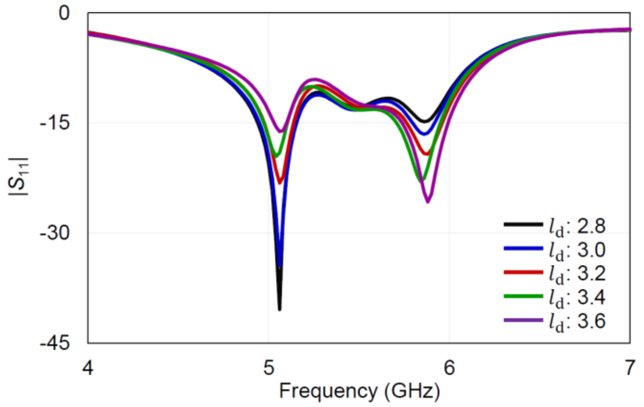

Figure 7. Effect of coupling feedline length (unit mm) on the performance of the proposed proximity-coupled patch antenna.

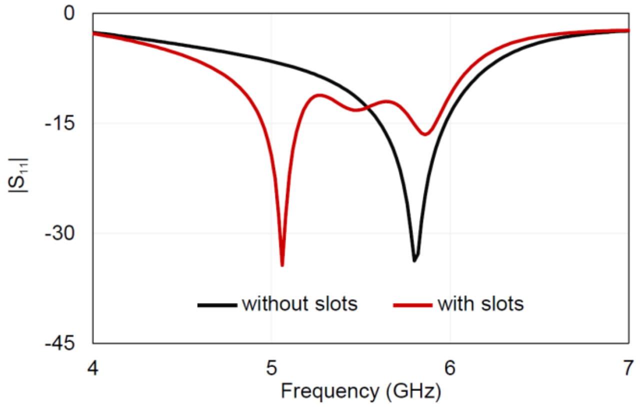

Figure 8. Frequency response and $|S_{11}|$ of the proposed proximity-coupled patch antenna.

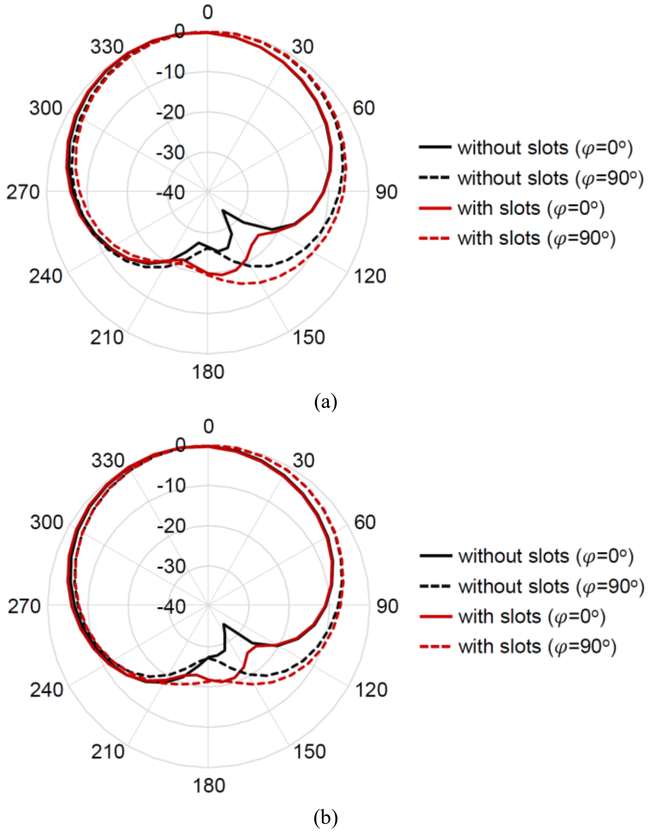

Figure 9. Normalized radiation patterns of the proposed proximity-coupled patch antenna, (a) 5.5 GHz, (b) 5.8 GHz.

TABLE II. PERFORMANCE COMPARISON WITH RELATED WORKS

Ref.	Antenna Type	Material	Bandwidth enhancement method	Center frequency (GHz)	Fractional bandwidth (%)	Peak gain (dBi)	Profile (λ_0)
[17]	Leaky-wave	FR-4	Slot and DGS	6.18	11.05	5.06	0.033
[18]	Dielectric resonator antenna	RO3035	Dual cavity-mode excitation	5.15	26	8.2	0.19
[19]	Slot	RT/duroid 5880	Air substrate and parasitic elements	5.7	23	2.9	0.044
[20]	Patch	RT/duroid 5880	Dual feedline and truncated	3.53	5.96	N/A	0.018
[21]	Patch	FR-4	Multi-resonant elements	5.5	18.5	4.8	0.03
This work	**Patch**	**FR-4**	**Proximity coupling and open-ended ring-shaped slots**	**5.4**	**22.3**	**2.6**	**0.06**

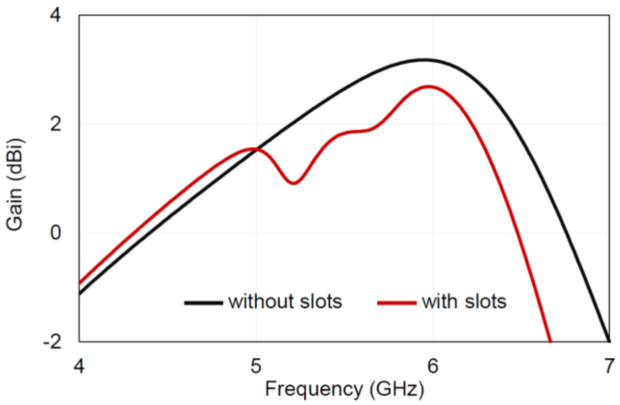

Figure 10. Gain of the proposed proximity-coupled patch antenna.

Furthermore, radiation patterns and gain are presented to demonstrate radiation characteristics of the antenna with and without slots. The radiation patterns are plotted at two different frequencies within the operating bandwidth of both proximity-coupled patch antennas, i.e., 5.5 GHz and 5.8 GHz. From the results, it is observed that the presence of slots slightly alters the radiation pattern of the antenna in the elevation plane (φ = 0° and φ = 90°). Even though there is a minor change in the back radiation, the proposed patch antenna maintains a stable radiation pattern at both frequencies, as depicted in Figure 9. In addition, as shown in Figure 10, the simulated boresight gain is 3.1 dBi and 2.6 dBi for the proximity-coupled patch antenna without and with slots, respectively. The slight degradation in gain performance is attributed to reduced radiation efficiency caused by the presence of slot structures on the radiating patch. This effect becomes more pronounced in the lower frequency region, where the slot element resonates.

B. Discussions

Performance comparison of the proposed patch antenna with related works is provided in Table II, where λ_0 represents the free-space wavelength corresponding to the antenna center frequency. In [17], slot and defected ground structure (DGS) were introduced for bandwidth enhancement of a leaky-wave antenna and could provide a fractional bandwidth of 11.05% with a high gain of 5.06 dBi. Meanwhile, a dielectric resonator antenna (DRA) with a wide bandwidth of 26% in the sub-6 GHz band was proposed using dual cavity-mode excitation [18]. However, the implementation of the DRA structure results in a relatively high-profile antenna. In the same frequency band, a wideband antenna was achieved using slots, near-field resonant parasitic elements, and an air gap between the substrate and the ground plane [19]. The use of parasitic elements causes the beam to tilt away from the boresight direction and requires careful adjustment of the air gap to avoid shifts in the resonant frequency.

In [20], a patch antenna configured using RT/duroid 5880 was proposed for 5G applications. The antenna provides a low-profile structure with a fractional bandwidth of 5.96% using a dual feedline and truncated configuration. A wideband patch antenna was also reported in [21] using multi-resonant elements, achieving a bandwidth of 18.5% while maintaining a low-profile structure. Compared with these works, the proposed antenna achieves a fractional bandwidth of 22.3% with a simple patch structure and relatively low profile, demonstrating its feasibility for wideband sub-6 GHz applications. To improve the antenna gain, a low-loss tangent substrate material could be employed in the existing structure, however, this would also result in changes to the antenna dimensions, particularly for materials with lower dielectric constants.

IV. CONCLUSION

Bandwidth enhancement of the patch antenna has been investigated through a simulation-based approach. The antenna is fed using a proximity-coupling method, with dual open-ended ring-shaped slots etched on the radiating patch. The results indicate that the integration of the indirect feeding method with proper tuning of the slot configuration enables a wide impedance bandwidth in the sub-6 GHz band while maintaining a stable radiation pattern. Although a slight reduction in boresight gain is observed due to radiation deficiencies caused by the slots, the antenna still provides adequate gain across the operating bandwidth. Experimental characterization of the design will be conducted in the near future to further demonstrate its feasibility, and the corresponding results will be published subsequently.

REFERENCES

[1] M. S. Akbar, Z. Hussain, M. Ikram, Q. Z. Sheng, and S. C. Mukhopadhyay, "On challenges of sixth-generation (6G) wireless networks: A comprehensive survey of requirements, applications, and security issues," *J. Netw. Comput. Appl.*, vol. 233, Art. no. 104040, 2025, doi: 10.1016/j.jnca.2024.104040.

[2] C. Kumar, S. K. Raghuwanshi, and V. Kumar, "Graphene based microstrip patch antenna on photonic crystal substrate for 5G application," *Front. Mater.*, vol. 9, Art. no. 1079588, 2022, doi: 10.3389/fmats.2022.1079588.

[3] C. M. Saleh, E. Almajali, S. S. Alja'afreh, and J. Yousaf, "Dual U-slot patch antenna for 5G applications," in *Proc. 2021 IEEE International Symposium on Antennas and Propagation and USNC-URSI Radio Science Meeting (APS/URSI),* 2021, pp. 349-350, doi: 10.1109/APS/URSI47566.2021.9703904.

[4] F. -C. Lutz, W. Keusgen, and B. Gashi. "Off-chip double U-shaped slot patch antenna for H-band applications," in *Proc. 2025 19th European*

Conference on Antennas and Propagation (EuCAP), 2025, pp. 1-4, doi: 10.23919/EuCAP63536.2025.10999853.

[5] H. Yuan, F. -C. Chen, and Q. -X. Chu, "A wideband and high gain dual-polarized filtering antenna based on multiple patches," *IEEE Trans. Antennas Propag.*, vol. 70, no. 10, pp. 9843-9848, 2022, doi: 10.1109/TAP.2022.3177494.

[6] W. Su, J. Li, and R. -H. Liu, "Compact double-layer wideband circularly polarized microstrip antenna with parasitic elements," *Int. J. RF Microw. Comput.-Aided Eng.*, vol. 31, no. 1, Art. no. e22471, 2021, doi: 10.1002/mmce.22471.

[7] Z. Khan, M. H. Memon, S. U. Rahman, M. Sajjad, F. Lin, and L. Sun, "A single-fed multiband antenna for WLAN and 5G applications," *Sensors*, vol. 20, no. 21, Art. no. 6332, 2020, doi: 10.3390/s20216332.

[8] C. Kumar and D. Guha, "Asymmetric and compact DGS configuration for circular patch with improved radiations," *IEEE Antennas Wirel. Propag. Lett.*, vol. 19, no. 2, pp. 355-357, 2020, doi: 10.1109/LAWP.2019.2962569.

[9] G. G. B. Öner, S. Başbuğ, and Y. Altuncu, "Design of a compact multilayer high-gain microstrip patch antenna for IoT applications," *J. Electromagn. Eng. Sci.*, vol. 25, no. 6, pp. 570-583, 2025, doi: 10.26866/jees.2025.6.r.323.

[10] C. Sahana, M. Nirmala Devi, and M. Jayakumar, "Hexagonal-triangular combinatorial structure based dual-band circularly polarized patch antenna for GAGAN receivers," *IEEE Access*, vol. 11, pp. 23205-23216, 2023, doi: 10.1109/ACCESS.2023.3252913.

[11] N. -W. Liu, L. Zhu, W. -W. Choi, and G. Fu, "A low-profile wideband aperture-fed microstrip antenna with improved radiation patterns," *IEEE Trans. Antennas Propag.*, vol. 67, no. 1, pp. 562-567, 2019, doi: 10.1109/TAP.2018.2878099.

[12] R. Mir, H. Dashti, and J. A-. Shokouh, "Design and analysis of circularly polarized circular patch antenna with multiple shorting pins using characteristic mode theory," *AEU-Int. J. Electron. Commun.*, vol. 146, Art. no. 154112, 2022, doi: 10.1016/j.aeue.2022.154112.

[13] K. Yang, M. Wang, and X. Jia, "Improved bandwidth of patch antenna using dual-layer metasurface," *Prog. Electromagn. Res. Lett.*, vol. 124, pp. 69-75, 2025, doi: 10.2528/PIERL24120601.

[14] A. Firdausi, G. Hendrantoro, E. Setijadi, and M. Alaydrus, "Analysis and improvement of bandwidth and gain of millimeter-wave microstrip Franklin antenna with proximity-coupled feed," *IEEE Access*, vol. 11, pp. 104723-104734, 2023, doi: 10.1109/ACCESS.2023.3317999.

[15] V. L. Pham, S. X. Ta, K. K. Nguyen, C. Dao-Ngoc, and N. Nguyen-Trong, "Single-layer, dual-band, circularly polarized, proximity-fed meshed patch antenna," *IEEE Access*, vol. 10, pp. 94560-94567, 2022, doi: 10.1109/ACCESS.2022.3204685.

[16] C. A. Balanis, *Antenna Theory: Analysis and Design*, 3rd ed. Hoboken, NJ, USA: John Wiley & Sons, Inc., 2005.

[17] F. Y. Zulkifli and M. W. Iqbal, "Bandwidth and gain enhancement of microstrip leaky-wave antennas with slot and defected ground structure," *J. Eng. Technol. Sci.*, vol. 55, no. 3, pp. 289-299, 2023, doi: 10.5614/j.eng.technol.sci.2023.55.3.6.

[18] R. S. Malfajani, J. -J. Laurin, and M. S. Sharawi, "Wideband substrate integrated cavity-backed dielectric resonator antenna at sub-6-GHz band," *IEEE Open J. Antennas Propag.*, vol. 4, pp. 60-68, 2022, doi: 10.1109/OJAP.2022.3231892.

[19] W. A. Khan, R. Raad, F. Tubbal, and P. I. Theoharis, "A compact broadband 5GHz IoT antenna," in *Proc. 2024 IEEE International Symposium on Antennas and Propagation and INC/USNC-URSI Radio Science Meeting (AP-S/INC-USNC-URSI)*, 2024, pp. 857-858, doi: 10.1109/AP-S/INC-USNC-URSI52054.2024.10686377.

[20] S. P. Marnel, D. W. Astuti, M. Alaydrus, and H. A. Majid, "Bandwidth enhancement of microstrip antenna with dual feed line and truncated for 5G applications," *Jurnal Rekayasa Elektrika*, vol. 21, no. 3, pp. 160-166, 2025, doi: 10.17529/jre.v21i3.44345.

[21] M. M. Ulfah and R. S. Asthan, "Wideband multi-resonant microstrip patch antenna for wireless communication systems," *Jurnal Teknik Elektro*, vol. 17, no. 2, pp. 51-56, 2025, doi: 10.15294/jte.v17i2.35545.